Available online at www.sciencedirect.com

jmr&t Journal of Materials Research and Technology

https://www.journals.elsevier.com/journal-of-materials-research-and-technology

Original Article

Leaching of iron and chromium from an indigenous ferro chromium alloy via a rotary evaporator: optimum conditions determination and kinetic analysis

Mehmet Feryat Gülcan[a], *Billur Deniz Karahan*[b,c,*], *Sebahattin Gürmen*[a]

[a] *Istanbul Technical University, Department of Metallurgical and Materials Engineering, 34469 Maslak-Istanbul, Turkey*
[b] *Istanbul Medipol University, Department of Civil Engineering, 34810 Beykoz-Istanbul, Turkey*
[c] *Istanbul Medipol University, Research Institute for Health Sciences and Technologies (SABITA), 34810 Beykoz-Istanbul, Turkey*

ARTICLE INFO

Article history:
Received 5 May 2020
Accepted 30 September 2020
Available online 17 October 2020

Keywords:
Leach
Ferro chromium alloy
Rotary evaporator
Taguchi method
Kinetic study

ABSTRACT

In the leaching process of chromium-containing precursor hexavalent chromium may form, which provokes damages to environment and human health. As a solution, leaching the chromium containing precursor with sulphuric acid to get chromium ions into solution without forming hexavalent ions has been proposed. These experiments are mostly carried out at high temperatures to increase the yield, while the detrimental effect of evaporation is still under investigation. In this study, indigenous ferro chromium alloys (>60 wt% Cr) have been leached with sulphuric acid by using a rotary evaporator where no evaporation occurs. The acid molarity, solid:liquid ratio, temperature and rotation rate of the rotary flask have been optimized using Taguchi method to maximize Fe and Cr dissolutions' efficiencies. Leaching in 5 M sulphuric acid solution with 1:50 solid:liquid ratio, at 90° C, 30 rpm for 150 min could sustain yields around 73% and 56% for Cr and Fe recoveries, respectively. Within the scope of this research, the effects of the mentioned parameters on the leaching efficiency have been also analyzed via the ANOVA method. The most effective parameters for Cr and Fe have been found as temperature and solid:liquid ratio, respectively. Finally, the kinetic has been also studied and universal equations have been successfully tested. $-\ln(1-x) = k^{*}t^{n}$ gives the best fitting result (where $n = 0.4$ and 0.6 are calculated for Fe and Cr, respectively). These values indicate that the leaching reaction follows the mixed kinetic control model. The activation energies are calculated as 46.12 kJ/mol for Fe and 142.8 kJ/mol for Cr.

* *Corresponding author.*
E-mail: bdkarahan@medipol.edu.tr (B.D. Karahan).

https://doi.org/10.1016/j.jmrt.2020.09.133

Nomenclature

CCC	Cross Correlation Coefficient
FeCr	ferrochromium
Wt.%	weight percentage
kJ/mol	kilojoule per mole
AAS	atomic absorption spectroscopy
S/L	solid/liquid ratio (vol./vol.)
SSE	sum of squared errors
vol.	volume
XRD	X-ray diffraction
XRF	X-ray fluorescence
S/N	signal to noise ratio
E_A	activation energy
R	gas constant

1. Introduction

Lately, environmental pollution caused by pyrometallurgical processes and increase in energy costs have led to the search for producing high value-added transition metal oxides powders by a cheaper, environmentally sensitive and practical method. Recently, Guo et al. [1] have proposed that the production of transition metal oxide (TMO) powders through a liquid phase presents outstanding advantages such as regulating morphology and size of the final powders. Therefore, instead of using synthetic production methods where high quality primary materials have been selected as precursor; it is believed that designing a process capable of leaching different transition metals from any type of precursor material may attract attention of large audience as the solution could be used in the TMO's powder production.

In this study, to set an example for this idea, a cheap, clean and practical process is proposed for obtaining a solution that contains transition metals ions (i.e. iron and chromium ions). In view of this, an indigenous ferro chromium alloy being widely used in refractory, chemical and steel industries has been particularly chosen as the precursor material. The reason for choosing ferro chromium alloy as the indigenous precursor is the fact that Turkey is a well-recognized producer of high quality ferro chromium in large quantities [2].

It is known that the choice of chemicals and experimental parameters to be used in such research are of critical importance as chromium tends to assume hexavalent value at high and low pH values of the solution. It is to be noted, these hexavalent chromium ions that harm the environment and human health are universally prohibited. Within this context, Lui et al. [3] have stated that sulphuric acid leaching of chromite ores prevents hexavalent chromium formation in the solution. In pursuit of that, Mohanty et al. [4] have leached a raw material containing 24% iron with various types of acids (HCl, H_2SO_4 and HNO_3), salt mixture (NaCl and $CuCl_3$) and bases (NaOH). They have revealed that 1.93 M sulphuric acid achieves the highest efficiency [4]. Subsequently, Tzeferis at al. [5] have leached lateritic nickel ore by organic acids, sulphuric acid and their mixtures. The outcomes have demonstrated the superiority of sulphuric acid to achieve the highest efficiency in leaching of transition metals. Later, researchers have investigated the effects of temperature, process duration, acid concentration, precursor particle size and solid:liquid ratio on transition metals' leaching efficiencies [3,6,7]. Therefore, to define the maximum leaching efficiency conditions, Taguchi method has been preferred similar to previous leaching studies [8–11] since it can predict contribution of each variable onto the outcome and permits optimization of numerous control factors with least number of trials. Thus, by using Taguchi method not only the cost and time are decreased, but also the quality is improved, eventually [12,13].

Within the scope of the paper, an indigenous ferro chromium alloy is leached with sulphuric acid to successfully transfer chromium and iron (as well as other trace amount of transition metals) into the solution as trivalent and divalent ions. During the experiments, a rotary evaporator is used for the first time to leach an indigenous ferro chrome alloy with 5% wt C content in contrast to traditional stirring options (such as mechanical and magnetic stirring). The rotary evaporator has been particularly chosen since in hydrometallurgical processing of chromium, pH adjustment and evaporation are important criteria to be considered to alleviate harm on environment and living creatures. It is expected that the change in the reactor type not only modifies the interaction between the active particles (ferro chromium alloys) and the leaching media (sulphuric acid) but also enhances the safety of the leaching process.

For the first time in the open literature, Taguchi experimental design technique and the ANOVA analysis have been used to maximize the leaching efficiency and analyze the parameters' effect on the leaching process when an indigenous ferro chromium alloy with 5%C content has been leached out with sulphuric acid in a rotary evaporator. To define the optimum process parameters, Taguchi orthogonal array method is applied via four parameters with three levels, as presented in Table 1. The control experiment has been run in addition to demonstrate the consistency and repeatability of the leaching experiments' results. Furthermore, a kinetic study is also realized to reveal the control mechanism of Fe and Cr dissolutions under the optimum sulphuric acid leaching conditions of the ferro chromium alloy.

2. Experimental

2.1. *Materials*

During the experiments, an indigenous ferro chromium alloy is used. Sulphuric acid is Merck Quality (1.00713.2500) and deionized water is of analytical grade. Ethanol is supplied by Merck (1.00983.2511).

2.2. *Ferro chromium preparation*

Prior to starting the leaching operation, ferro chromium chunks are milled to reduce grain size, in order to increase the solid/liquid (acid) interaction during leaching. Particles with grain size under 140 mesh are milled for 4 h at 235 rpm by planetary ball mill (Retsch PM 100). 5 ml ethanol is used as dispersant. In the ball milling, zirconium oxide balls with 5 mm

Table 1 – Experiment levels for Taguchi orthogonal method L_9 (3^4).

Parameters	Units	First level	Second level	Third level
Molarity	(M)	0.5	2	5
Solid:liquid ratio	(vol:vol.)	1:50	1:100	1:200
Temperature	(°C)	25	60	90
Rotation rate of the flask	(rpm)	30	100	200

diameter are employed. During the experiments, ball/powder ratio is fixed as 10:1 in weight. Then, milled powders are cleansed at 60 °C for 4 h with 500 rpm in a magnetic stirrer to remove water soluble species from the precursor.

2.3. *Leaching procedure*

All leaching experiments have been done in a rotary evaporator system (Buchi Rotavapor® R-300). To optimize the leaching process parameters, nine experiments are designed via Taguchi orthogonal array method. Four parameters with three levels ($L_9(3^4)$) have been investigated: Molarity (0.5 M, 2 M and 5 M), volumetric solid: liquid ratio (1:50, 1:100 and 1:200), temperature (25 °C, 60 °C and 90 °C) and rotation rate of the flask (30, 100 and 200 rpm). The leaching duration (150 min) is kept constant for these nine experiments. The parameters and their levels are given in Table 1. After Taguchi and ANOVA analyses, an additional control experiment has been done at the optimum parameters to achieve maximum leaching efficiency of iron and chromium within the defined experimental frame. Finally, the effects of process duration as well as the stirring rate of the flask on the leaching efficiency have been investigated and kinetic calculations have been made to discuss the leaching controlling mechanisms of Fe and Cr, respectively.

2.4. *Chemical, morphological and structural analyses*

Chemical composition of the ferro chromium alloy and the solid residue remained after leaching have been analyzed by X-ray fluorescence (XRF, Hitachi X-MET8000, Malvern Panalytical – Epsilon1) and Energy Dispersive X-ray spectrometer (EDS, Bruker). Carbon and sulphur content of the precursor material (after cleansing) are determined by Eltra CS 800. For determining the recoveries of iron and chromium in the leaching solution, atomic absorption spectroscopy (AAS, Shimadzu AA 160) is used. In sampling, to keep the solid/liquid ratio as stable, each time 5 ml of leachate is taken for AAS analysis and right after 5 ml of sulphuric acid solution (with the same molarity) is added into the leachate at the same temperature. The taken samples are diluted via deionized water before the AAS analysis. The recovery of metals are calculated based on Eq. (1) [14];

$$\text{Recovery}\,(\%) = \frac{(\text{Metal in solution from AAS (g/L)}) * (\text{Leachate volume (L)})}{(\text{Metal amount in Fe} - \text{Cr(\%) from XRF}) * (\text{Initial Fe} - \text{Cr amount (g)})} * 100 \quad (1)$$

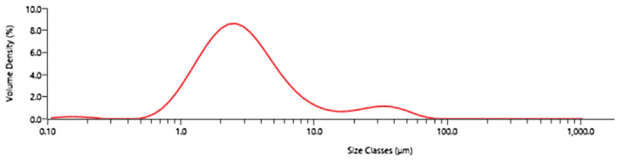

Fig. 1 – Particle size distribution of milled ferro chromium.

Investigation on particle size distribution and morphology have been made by Malvern–Mastersizer 3001 and scanning electron microscope (Zeiss Gemini 500), respectively. The structures of the precursor alloy and the residue have been characterized by X-ray diffraction method (XRD, Bruker AXS/Discovery D8) using Cu Kα as the X-ray sources (0.02°/s, between $2\theta = 15°–90°$).

Finally, the presence of Cr^{6+} in the leaching solution has been tested using the Colorometric analysis method (Standard Methods – 3500–Cr.B) [15]. All chemicals used for this experiment are of analytical reagent grade. A hexavalent chromium (Cr^{6+}) containing stock solution of 100 ml volume is prepared by dissolving 141.4 mg of potassium dichromate ($K_2Cr_2O_7$) in distilled water. Then 1 ml of this stock solution is diluted to 100 ml by using DI water. This sample is named as CRM during the analysis. In another volumetric flask, distilled water is added (as transparent solution) and named as BLANK. Finally, the FeCr leaching solution is diluted 100 times and added into another volumetric flask, the latter is named as NUM. The colour chelating agent used for this analysis is 1,5-diphenylcarbazide (DPC, Special Grade, Merck). During the analysis, the steps defined in the standard are followed.

3. Results and discussion

3.1. *Materials*

The chemical composition of the precursor material has been determined by XRF (Table 2) and EDS analyses. The results show that ferro chromium alloy contains a high amount of chromium (~68%) and iron (~29%) with trace amount of other transition metals such as Mn, Co and Ni.

An additional experiment has been conducted to determine the carbon content of the powder. The result reveals that the indigenous alloy contains ~5 wt.% carbon.

The particle size analysis of the ferro chromium alloy, after the ball milling, shows that an average particle size (Dv50) of 2.78 μm is achieved, eventually (Fig. 1). SEM images of the milled powder justify the particle size analysis' result and reveal an irregular morphology, as expected (Fig. 2) [16].

Table 2 – XRF analysis of an indigenous ferro chromium alloy and the residue after leaching (el.%).

	Fe	Co	Ni	Si	Cr	Other
Precursor	29.49	0.08	0.54	0.66	68.34	Balance
Residue	14.479	0	0.417	8.77	52.235	Balance

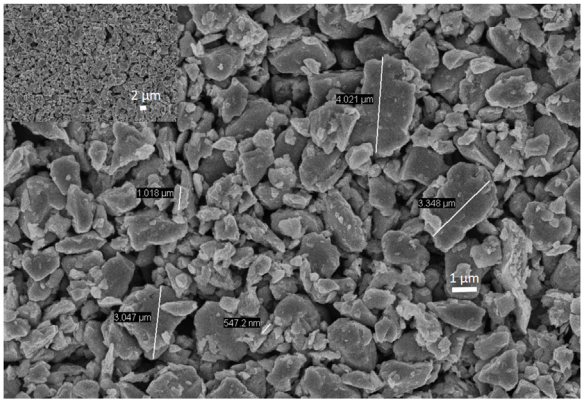

Fig. 2 – SEM images of the ball milled ferro chromium alloy 10,000× magnification (4 h, 235 rpm, 10:1 BPR) (SEM image at smaller magnification (5000×) in upper left-hand is given).

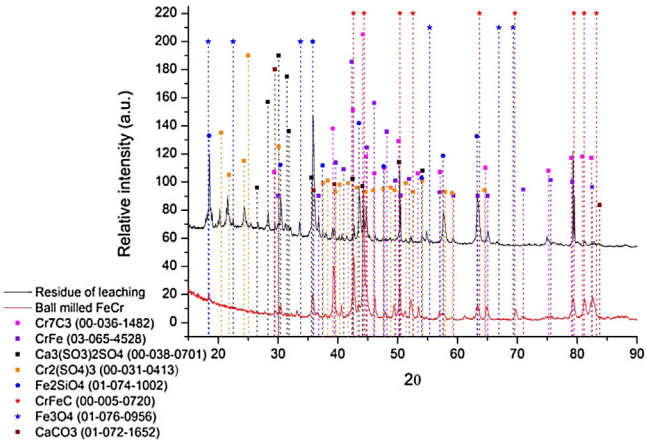

Fig. 3 – XRD pattern of the precursor ferro chromium alloy (red line) and the residue after leaching (black line). (For interpretation of the references to color in this figure legend, the reader is referred to the web version of this article.)

XRD result of the precursor material shows that the main sources of iron in the ferrochromium are CrFe (03-065-4528), CrFeC (00-005-0720), Fe_2SiO_4 (01-074-1002) and Fe_3O_4 (01-076-0956). And the main sources for chromium are CrFe, CrFeC and Cr_7C_3 (00-036-1482) as given in Fig. 3. All those compounds are commonly encountered species during the characterization of the high carbon-ferro chromium alloy [17–21]. Moreover, a small amount of calcium carbonate (01-072-1652) is detected in high carbon contained ferro chromium alloy which is originated from the production process, as described by Neizel et al. [18]

3.2. *Leaching reactions of the ferro chromium with sulphuric acid*

FeCr is found to be highly resistant to sulfuric acid leaching. Capilla and Delgado [22] claim that when the leaching occurs at 200 °C, it leads sulphate based precipitate formation following the Eq. (2). Then Nadirov et al. [23] have proposed that at high temperature (>80 °C) sulfuric acid leaching, fayalitic dissolution may happen following Eq. (3). Then, Salmimies et al. [24] have studied the sulfuric acid leaching of magnetite and indicated that magnetite has relatively high resistance to sulfuric acid leaching (Eq. (4)). Finally, carbides being a good refractor are known to be resistant to sulfuric acid leaching as stated by Kuznetsov et al. [25]. Herein, it is also important to mention that calcium carbonate that is present in the precursor transforms into calcium sulphate following the Eq. (5), as suggested by Havlik et al. [26].

Moreover, Liu et al. [14] have defined the sulphuric acid reaction of the trace amount of other transition metals (Ni, Co) that are present in the precursor (as detected by XRF), following Eqs. (6) and (7).

The possible reactions that may occur during the interaction of the precursor material (ferro chromium) with sulphuric acid are described below (see Eq. (2)–(7)) [14,23–28];

$$CrFe + H_2SO_4 \rightarrow FeSO_4 + Cr_2(SO_4)_3 + H_2 \quad (2)$$

$$2FeO * SiO_2 + 2H_2SO_4 \rightarrow 2FeSO_4 + H_4SiO_4 \quad (3)$$

$$Fe_3O_4 + 4H_2SO_4 \rightarrow FeSO_4 + Fe_2(SO_4)_3 + 4H_2O \quad (4)$$

$$CaCO_3 + H_2SO_{4(aq)} \rightarrow CaSO_4 + CO_2 + H_2O \quad (5)$$

$$H_2SO_4 + Co \rightarrow CoSO_4 + H_2 \quad (6)$$

$$H_2SO_4 + Ni \rightarrow NiSO_4 + H_2 \quad (7)$$

Additional characterization to detect hexavalent chromium existence in the leaching solution is done (see Supplementary file). The colour of the FeCr leaching solution (named as 'NUM') is detected to be between green and blue, which is similar to other trivalent solutions given in the literature [29] and different than the synthetically prepared Cr^{6+} solution (named as 'CRM', pink in colour). This observation can be explained by the fact that the Cr^{3+} in the leaching solution cannot be oxidized to a different valence state due to the insufficient oxidation potential of sulphuric acid, as stated previously by Geveci et al. [30].

3.3. *Taguchi experimental analysis of leaching process*

Nine different experiments have been designed following Taguchi's orthogonal array. The parameters and the level of

Table 3 – The parameters and the results of experiments based on L_9 (3^4) Taguchi's orthogonal arrays.

Experiments No.	Molar of acid solution (M)	Solid:liquid ratio (vol.)	Temperature (°C)	Rotation rate of the flask (rpm)	AAS Fe (g/L)	S/N for Fe (db)	AAS Cr (g/L)	S/N for Cr (db)
1	0.5	1:50	RT	30	10.81	20.67	18.15	25.18
2	0.5	1:100	60	100	9.59	19.64	10.16	20.14
3	0.5	1:200	90	200	9.1	19.19	28.32	29.04
4	2	1:50	60	200	12.38	21.86	36.64	3128
5	2	1:100	90	30	10.82	20.68	36.64	31.28
6	2	1:200	RT	100	7.04	16.95	4.99	13.97
7	5	1:50	90	100	13.1	22.35	38.31	31.67
8	5	1:100	RT	200	9.35	19.42	13.83	22.81
9	5	1:200	60	30	10.03	20.03	31.65	30.01

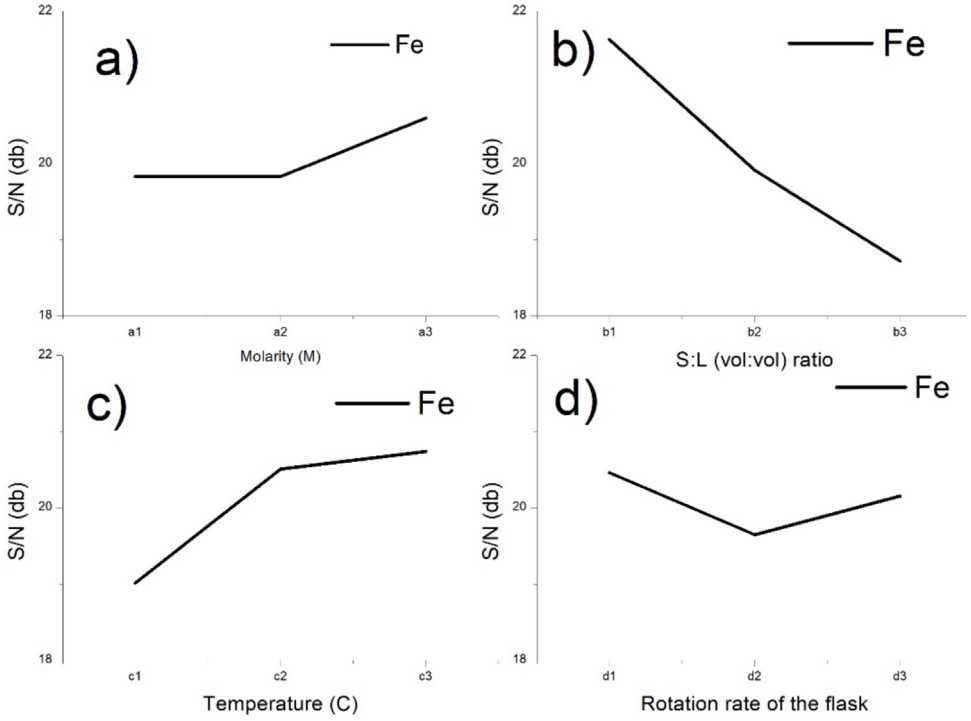

Fig. 4 – S/N values for iron of (a) molarity (M); (b) S:L (ml:ml) ratio; (c) temperature (°C); (d) rotation rate of flask (rpm).

each experiment with AAS analysis' result have been presented in Table 3. In leaching operation, the amount of metal ions is desired to be maximized. Thus, "larger is better" approach is chosen, accordingly. S/N ratios are calculated using the Eq. (8), where n represents the total number of replications of each test run; y represents the extraction yield of metals (chromium and iron) achieved in each experiment [32–33]. The S/N curvatures for all parameters in case of iron and chromium have been given in Figs. 4 and 5(a–d), respectively.

$$S/N = -10 * \log\left(\frac{1}{n} * \sum_{n}^{i=0}\left(\frac{1}{y_i^2}\right)\right) \quad (8)$$

Analysis of Variance (ANOVA) is used to identify the effect of each parameter on the metal extraction yields. The most effective parameters on Cr leaching are revealed to be: temperature and rotation rate of the flask (Tables 4 and 5). On the other hand, the most effective parameters on Fe leaching are revealed to be: solid:liquid ratio (vol:vol) and temperature (Tables 6 and 7).

When the leaching efficiencies of chromium and iron from the indigenous alloy have been calculated, ~73% and ~56% have been determined, respectively. These values have been determined by using AAS results, according to Eq. (1). This equation is used in Lui et al. [14] work and El bar et al. [7] work, previously.

Then, by using Eq. (9) a theoretical calculation about the Fe and Cr recoveries based on Taguchi approach is done. "T" refers to the average S/N ratios of all experiments, 'C' demonstrates the estimated S/N value related to the optimum leaching conditions. a_3, b_1, c_3 and d_1 are chosen as they are the levels of parameters to get maximum amount of metal ions into the solution (Figs. 4 and 5). The estimated value (C) is calculated as 23.165 db and 35.56 db for Fe and Cr, respectively. These correspond to 14.43 and 84.81 g/L Fe and Cr ions in the leach-

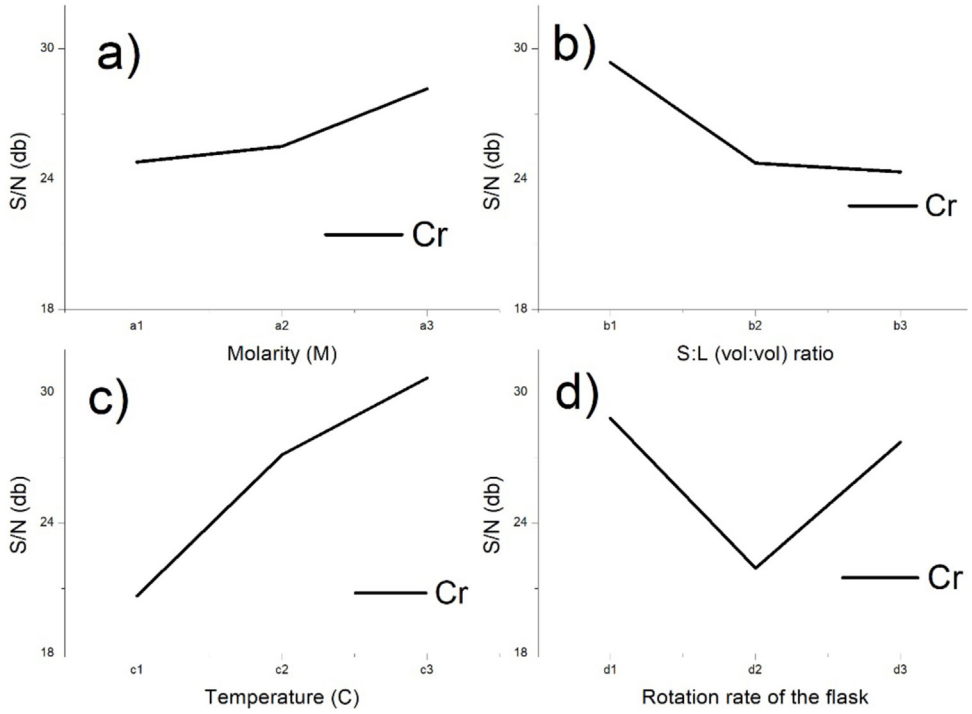

Fig. 5 – S/N values for chromium of (a) molarity (M); (b) S:L (ml:ml) ratio; (c) temperature (°C); (d) rotation rate of flask (rpm).

Table 4 – ANOVA analysis of chromium's leaching from ferro chromium alloy.

Parameter	Degree of freedom	Sum of square	Mean of square	F value
Molarity	2	18.95		
Solid:liquid	2	46.97		
Temperature	2	154.59		
Rotation rate of the flask	2	82.26		
Error				
Total	8	302.76		

Table 5 – Revised ANOVA analysis of chromium's leaching from ferro chromium alloy.

Parameter	Degree of freedom	Sum of square	Mean of square	F value
Temperature	2	154.59	77.30	4.69
Rotation rate of the flask	2	82.26	41.13	2.50
Error	4	65.91	16.48	
Total	8	302.76		

Table 6 – ANOVA analysis of iron's leaching from ferro chromium alloy.

Parameter	Degree of freedom	Sum of square	Mean of square	F value
Molarity	2	1.17		
Solid:liquid	2	12.78		
Temperature	2	5.26		
Rotation rate of the flask	2	1.02		
Error				
Total	8	20.22		

Table 7 – Revised ANOVA analysis of iron's leaching from ferro chromium alloy.

Parameter	Degree of freedom	Sum of square	Mean of square	F value
Solid:liquid	2	12.78	6.39	11.73
Temperature	2	5.26	2.62	4.82
Error	4	2.18	0.54	
Total	8	20.22		

ing solution, respectively. An additional control experiment is conducted at 90 °C, 30 rpm, 1:50 volumetric solid:liquid ratio (vol:vol), in 5 M sulphuric acid solution, for 150 min to confirm the experimental results. Fe and Cr concentrations in the control experiment's solution are detected as 13.22 ± .1.3 g/L and 39.0 ± .0.82 g/L, respectively.

$$C = T + (a_3 - T) + (b_1 - T) + (c_3 - T) + (d_1 - T) \quad (9)$$

The correlations between the numerical values obtained in pursuit of Eq. (9) and AAS results are found to be 46% for chromium and 92% for iron. These values have harmony with characterizations results and the outcomes given in the open literature [33–36].

As stated previously, the high resistance of intermetallic and carbide particles to sulphuric acid leaching could explain this observation. Meanwhile, low leaching kinetic of chromium in sulphuric acid as well as possible formation of chromium sulphate particles during leaching process could represent other reasons [31]. By the same token, Geveci et al. [30] have stated that lost in leaching efficiency of chromium can be attributed to the formation of stable chromium sulphate layer over the chromium particles during sulphuric acid leaching. To justify our hypothesis XRD analysis of the residue has been carried out (see Fig. 3, black line). XRD result of the residue showing the presence of chromium sulphate ($Cr_2(SO_4)_3$) verifies the reaction given as Eq. (2). Moreover, the presences of CrFeC, Cr_7C_3, Fe_3O_4, Fe_2SiO_4 and CrFe in the residue substantiate the fact that some amount of intermetallics, carbide and oxide (CrFeC, Cr_7C_3, Fe_3O_4, Fe_2SiO_4 and CrFe) have dissolved, some remain without being leached [25,31,37].

Chromium sulphate peaks identified in XRD results indicate the formation of a new phase as a result of leaching. Previous work on sulphuric acid leaching of chromium containing particles reveal that upon the leaching reaction chromium sulphate forms and covers the particle surface [30].

When comparing the residue's and the precursor's XRF analyses Ca amount is always found to be less than 1% both in the precursor and the residue (Table 2). And, the amount of Fe, Cr, Ni, Co are noted to be decreased from the precursor to the residue due to the dissolution reactions indicated in Eqs. 2–7. On the other hand, sulphur content is found to be increased after leaching operation (from 452 ppm to 14.095%el.) following the sulphate particles' formation, which is believed to negatively affect the leaching kinetic [28–30].

Further discussion on the independent parameters' effect on Fe and Cr leaching efficiencies is done based on Figs. 4 and 5. Figs. 4a and 5a reveal that the S/N ratios of molarity for leaching of iron and chromium reveal similar trends: first a slight then a remarkable improvement is noted when acid molarity is increased from 0.5 to 2 M, then 2 M to 5 M. Ige et al. [6] have reported a similar result and claimed that iron ion concentration in the leachate is increased in more concentrated sulphuric acid solutions. This fact is also valid for chromium leaching where higher chromium ion concentration is detected in more concentrated sulphuric acid solutions [6,14].

On the other hand, solid:liquid ratio is found to be inversely interacting with the leaching efficiencies of both iron and chromium, as expected: higher solid amount meaning more available material to be leached out, which results in higher leaching efficiency, eventually (Figs. 4b, 5b).

Figs. 4c, 5c demonstrate that temperature has a positive correlation with the iron and chromium concentrations in the leachate. An increase in temperature (from 25 °C to 90 °C) promotes the activity of atoms and molecules in the leachate as stated in previous studies [6,14], leading in an increase in the leaching efficiencies.

Finally, the rotation rate of the flask in the rotary evaporator system first decreases (from 30 to 100 rpm) then increases (from 100 to 200 rpm) the leaching efficiencies of iron and chromium. Possible changes at the solid/liquid interface upon leaching and deterioration of chromium sulphate layer over the particles might explain this performance.

3.4. *Kinetic analysis of ferro chromium's leaching*

Once the optimum parameters have been determined to maximize the leaching efficiencies of iron and chromium (5 M, 1:50 s:l (vol:vol) ratio, 90 °C, 30 rpm and 150 min), additional experiments have been run to kinetically investigate the process.

First, an experiment at the optimum conditions defined by Taguchi has been performed for 360 min to observe the change in metal recoveries of Cr (red line in Fig. 6b) and Fe (black line in Fig. 6a) upon the leaching duration. During the experiment, 12 samples have been taken out of the leaching solution at different time lapse (0, 1, 5, 15, 60, 90, 120, 150, 180, 240, 300 and 360 min). Both Cr and Fe recoveries have been noted to rapidly increase in the first 60 min of leaching, then roughly get stabilized after 150 min. A scrutiny look in Fig. 6a and b reveal that in the first 15 min. of the leaching reaction, the efficiencies increase exponentially, then between 15 and 60 min the efficiencies rise with different slopes, and finally from 60 to 150 min fluctuations in the recoveries with a positive slope are observed in Fig. 6a and b. This trend is very similar to what has been stated in the literature [38]. Ruiz et al. [38] have classified this type of leaching kinetic in three parts: induction, conversion and stabilization. They have explained that the induction is the shortest period lasting around 20 min and afterwards the conversion has taken place where metal complexing happened in the solution, and lastly at the stabilization, leaching operation ended with its highest recovery efficiency [38].

Noting that leaching is a heterogeneous reaction that occurs between solid and liquid phases, the reaction begins primarily at the powder/acid solution interface and the dissolution progressively occurs by reducing the size of the powder. Therefore, for the leaching process of the ferro chromium alloy (with 5% C content), as agreed with Sokic et al.'s [39] study, not only the chemical reaction of sulphate ions with the powder, but also the diffusion of lixiviant species should be considered to explain the mechanism. Considering this fact, the universal formula used for kinetic modelling of leaching reaction are reviewed and the R^2 (Table 8) values and Cross Correlation Coefficient (CCC) (Table 9) values of Cr and Fe recoveries at different temperatures are calculated according to Şen [44]. Herein x, a, t and n stand for metal fraction, initial metal amount, time (min) and constant values.

The maximum values of R^2, R^2_{adj} and CCC for Fe and Cr dissolution, are achieved when the 'mixed kinetic control' model

Table 8 – Kinetic models and the calculated R^2, adjusted R^2 and mean of squares values for Cr and Fe leaching.

Expression	Controlling mechanism	R^2 (adjusted R^2)						SSE						
		Fe 45 °C	Fe 60 °C	Fe 90 °C	Cr 45 °C	Cr 60 °C	Cr 90 °C	Fe 45 °C	Fe 60 °C	Fe 90 °C	Cr 45 °C	Cr 60 °C	Cr 90 °C	Ref.
$1-\frac{2}{3}*x-(1-x)^{\frac{2}{3}}=k*t^n$	Diffusion through product layer	0.617 (0.5532)	0.8582 (0.8346)	0.6426 (0.583)	0.6408 (0.5809)	0.9241 (0.9114)	0.7384 (0.6948)	0.002863	0.003698	0.007638	0.000704	0.003394	0.01658	[40]
$\ln(a/a\text{-}x)=k^*t^n$	Chemical reaction control model	0.6766 (0.6227)	0.942 (0.9323)	0.8045 (0.772)	0.762 (0.7226)	0.994 (0.9929)	0.8992 (0.8824)	0.000163	0.000561	0.005114	0.000001	0.000007	0.001160	[41]
$-\ln(1-x)=k*t^n$	Mixed model (surface reaction control; lixiviant diffusion model)	0.6784 (0.6248)	0.9392 (0.9290)	0.8357 (0.8083)	0.763 (0.7235)	0.9945 (0.9936)	0.9363 (0.9256)	0.001201	0.005271	0.04945	0.000031	0.000299	0.05841	[39]
$1-(1-x)^{\frac{1}{3}}=k*t^n$	Chemical reaction control	0.6755 (0.6237)	0.9409 (0.9310)	0.8213 (0.7915)	0.762 (0.7231)	0.9944 (0.9935)	0.9232 (0.9104)	0.000130	0.000503	0.004668	0.000003	0.000031	0.005820	[42]
$1-(1-0.45*x)^{\frac{1}{3}}=k*t^n$	Surface reaction control by shrinking core model	0.6764 (0.6225)	0.9421 (0.9324)	0.802 (0.769)	0.7623 (0.7227)	0.9941 (0.9931)	0.9044 (0.8884)	0.000026	0.000087	0.000785	0.000001	0.000006	0.001038	[43]
$1-(1-x)^{\frac{2}{3}}=k*t^n$	Shrinking core model (Film diffusion control-dense-shrinking model)	0.6726 (0.618)	0.9387 (0.9285)	0.7398 (0.6964)	0.7610 (0.7212)	0.9912 (0.9898)	0.8464 (0.8208)	0.000468	0.001159	0.008566	0.000014	0.000141	0.01272	[42]

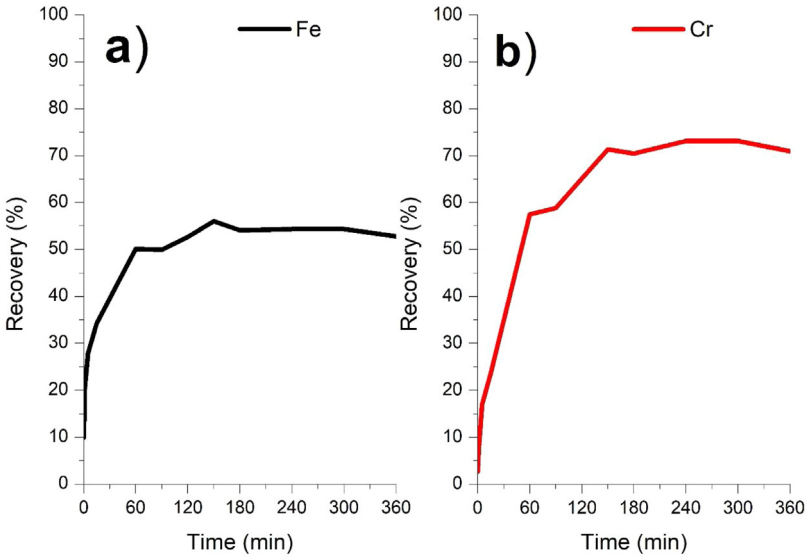

Fig. 6 – Recovery-time graphs of (a) iron and (b) chromium.

Table 9 – Kinetic models and the calculated CCC values for Cr and Fe leaching.

Expression	Controlling mechanism	Fe 45 °C	Fe 60 °C	Fe 90 °C	Cr 45 °C	Cr 60 °C	Cr 90 °C	Refs.
$1-\frac{2}{3}*x-(1-x)^{\frac{2}{3}}=k*t^n$	Diffusion through product layer	0.6875	0.8106	0.7013	0.7002	0.8411	0.7518	[40]
$\ln(a/a\text{-}x)=k^*t^n$	Chemical reaction control model	0.7209	0.8494	0.7850	0.7643	0.8723	0.8297	[41]
$-\ln(1-x)=k^*t^n$	Mixed model (surface reaction control; lixiviant diffusion model	0.7207	0.8480	0.7999	0.7650	0.8726	0.8467	[39]
$1-(1-x)^{\frac{1}{3}}=k*t^n$	Chemical reaction control	0.7211	0.8488	0.7930	0.7617	0.8726	0.8407	[42]
$1-(1-0.45*x)^{\frac{1}{3}}=k*t^n$	Surface reaction control by shrinking core model	0.7206	0.8493	0.7834	0.7679	0.8725	0.8321	[43]
$1-(1-x)^{\frac{2}{3}}=k*t^n$	Shrinking core model (Film diffusion control-dense-shrinking model)	0.7175	0.8478	0.7526	0.7599	0.8712	0.8050	[42]

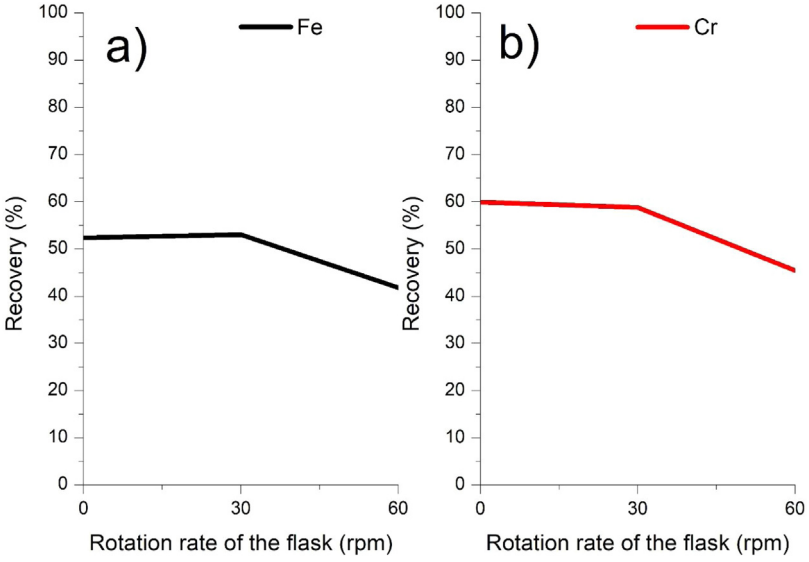

Fig. 7 – Recovery-rotation rate of the flask graphs of (a) iron and (b) chromium.

Table 10 – Calculated R^2, R^2adj and SSE values for different n (n = 1-0.3) in kinetic expression of this study.

n values	R^2 (R^2 adj)								SSE							
	Fe 45 °C	Fe 60 °C	Fe 90 °C	Cr 45 °C	Cr 60 °C	Cr 90 °C	Average of Fe	Average of Cr	Fe 45 °C	Fe 60 °C	Fe 90 °C	Cr 45 °C	Cr 60 °C	Cr 90 °C	Average of Fe	Average of Cr
1	0.6784 (0.6248)	0.9392 (0.9290)	0.8357 (0.8083)	0.763 (0.7235)	0.9945 (0.9936)	0.9363 (0.9256)	0.8178 (0.7874)	0.8979 (0.8809)	0.001201	0.005271	0.04945	0.000031	0.000299	0.05841	0.0186	0.0196
0.9	0.6921 (0.6491)	0.9356 (0.9249)	0.8594 (0.8360)	0.7720 (0.734)	0.9939 (0.9929)	0.9514 (0.9433)	0.8290 (0.8033)	0.9058 (0.8901)	0.001150	0.005576	0.04230	0.000030	0.000330	0.04455	0.0163	0.0150
0.8	0.7078 (0.6591)	0.9306 (0.9191)	0.8841 (0.8648)	0.7819 (0.7455)	0.9905 (0.9889)	0.9650 (0.9592)	0.8408 (0.8143)	0.9125 (0.8979)	0.001091	0.006010	0.03488	0.000028	0.000517	0.03204	0.0140	0.0109
0.7	0.7259 (0.6803)	0.9238 (0.9111)	0.9095 (0.8944)	0.7928 (0.783)	0.9833 (0.9805)	0.9764 (0.9725)	0.8531 (0.8286)	0.9175 (0.9120)	0.001023	0.006604	0.02723	0.000027	0.000909	0.02163	0.0116	0.0075
0.6	0.7470 (0.7048)	0.9143 (0.9001)	0.9353 (0.9246)	0.8049 (0.7724)	0.9708 (0.9660)	0.9841 (0.9814)	0.8655 (0.8432)	0.9199 (0.9066)	0.000945	0.007423	0.01946	0.000025	0.001588	0.01459	0.0093	0.0054
0.5	0.7710 (0.7329)	0.9008 (0.8842)	0.9605 (0.9539)	0.8176 (0.7872)	0.9503 (0.9421)	0.9854 (0.983)	0.8774 (0.8570)	0.9178 (0.9041)	0.000855	0.008598	0.01188	0.000024	0.002702	0.01334	0.0071	0.0054
0.4	0.7967 (0.7629)	0.8795 (0.8594)	0.9818 (0.9788)	0.8282 (0.7996)	0.9164 (0.9024)	0.9749 (0.9707)	0.8860 (0.8670)	0.9065 (0.8909)	0.000759	0.01044	0.005472	0.000108	0.004551	0.02301	0.0056	0.0092
0.3	0.8178 (0.7974)	0.8409 (0.8144)	0.9893 (0.9875)	0.8282 (0.7998)	0.8564 (0.9325)	0.9391 (0.929)	0.8827 (0.8654)	0.8746 (0.8871)	0.000681	0.01378	0.003216	0.000022	0.007814	0.05580	0.0059	0.0212

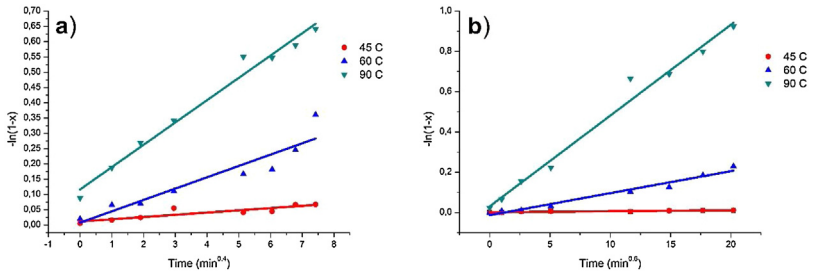

Fig. 8 – Kinetic curves of sulphuric acid leaching of (a) iron; (b) chromium.

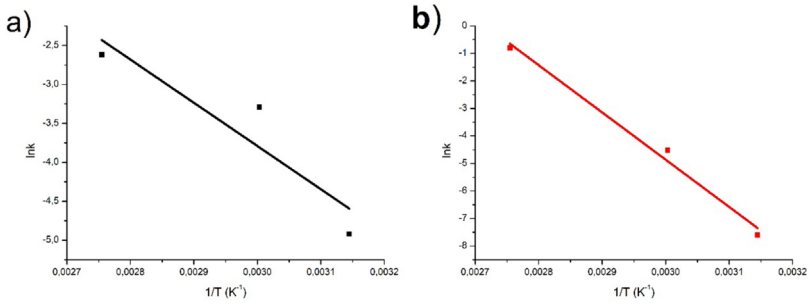

Fig. 9 – ln *K* – 1/*T* plots (a) iron; (b) chromium.

is used ($n = 1$). Additionally, SSE values are also calculated (see Table 8). The results agree with the literature's outcome and confirm that [39] both surface reaction and lixiviant diffusion to solid particles are important in leaching of ferro chromium alloy. To further support this observation, experiments at the optimum leaching conditions with different flask's rotation rates (0, 30 and 60 rpm) have been conducted (Fig. 7a and b). The stagnant acid solution yields the worst efficiency. Such behaviour has been also observed in Lui et al.'s [14] work. Fig. 7a and b demonstrate that the difference in the leaching efficiencies (recovery %) at the different flask's rotation rates is always lower than 40%, which substantiates the effect of chemical reaction on leaching [39] mechanism.

To evaluate the leaching mechanism in detail, fitting of kinetic model could be made by modifying n value in the formula $-\ln(1-x) = k * t^n$. If n is near to 1, the reaction is described as an ideal chemical reaction control, then when n value is equal to or lower than 0.5 diffusion control mechanism overcomes. The calculations demonstrate that the highest average R^2 (and R^2_{adj}) and CCC values (for 45 °C, 60 °C and 90 °C) are achieved when $n = 0.4$ is used (R^2: 0.886) for iron (Fig. 8a), and $n = 0.6$ is utilized for (Avergaer A R^2: 0.9199) chromium leaching (Fig. 8b) which could be seen in Table 10.

Further, activation energy of each leaching reaction is calculated based on Arrhenius equation (Eq. (10)). E_A, R and T stand for activation energy (kJ/mol), gas constant (8.314 J/mol K) and temperature (K) respectively.

$$\ln K = \ln A - \frac{E_A}{R * T} \tag{10}$$

Following Eq. (10) the activation energies are calculated as 46.12 kJ/mol and 142.8 kJ/mol for iron and chromium leaching (Fig. 9), respectively. These energy values show resemblance with the activation energies reported in the open literature [14,36,45].

4. Conclusion

The outcomes of this study can be summarized as follows:

- For the first time in the open literature, an indigenous ferro chromium alloy with 5%C content is leached with sulphuric acid in a rotary evaporator system.
- The optimization of the leaching process is achieved by Taguchi experimental design. Then, further kinetic analysis is realized to discuss the leaching mechanism in detail.
- The highest efficiency is achieved when FeCr alloy is leached in 5 M sulphuric acid solution with 1:50 volumetric solid:liquid ratio at 90 °C for 150 min, with a flask rotation speed of 30 rpm. Leaching efficiencies of iron and chromium are found to be ~56% and ~73%, respectively. The reason of such efficiency is believed to be related to the existence of carbides (CrFeC, Cr_7C_3,), iron silicon oxide (Fe_2SiO_4) and CrFe intermetallics in the precursor and the formation of chromium sulphate ($(Cr_2(SO_4)_3$) particles during leaching process.
- ANOVA analysis reveals that volumetric solid:liquid ratio (vol:vol) and temperature are important parameters for iron leaching; whereas in the case of chromium leaching, rotation rate of the flask and temperature are found to be significant parameters.
- The kinetic investigation of ferro chromium leaching shows that both leaching of iron and chromium have been controlled by surface reaction and lixiviant diffusion through solid particles. Activation energies for each leaching process

are calculated to be: 46.12 kJ/mol for iron and 142.8 kJ/mol for chromium.

Conflicts of interest

The authors declare that they have no known competing financial interests or personal relationships that could have appeared to influence the work reported in this paper.

Acknowledgements

The authors would like to greatly acknowledge TUBITAK/Turkey (Project No: 218M768) for financial support. The authors thank Eti Krom A.Ş. for supplying the alloy. The authors thank Prof. Dr. Süheyla Aydın, Prof. Dr. Özgül Keleş (Istanbul Technical University) and Onur Çetin (Arçelik Global) for their helps in characterizations.

Appendix A. Supplementary data

Supplementary data associated with this article can be found, in the online version, at doi:10.1016/j.jmrt.2020.09.133.

REFERENCES

[1] Guo T, Yao MS, Lin YH, Nan CW. A comprehensive review on synthesis methods for transition-metal oxide nanostructures. Cryst Eng Commun 2015;17(19):3551–85, http://dx.doi.org/10.1039/C5CE00034C.
[2] Boğazliyan M. Time series analysis of Turkish exports of selected ores and concentrates. Middle East Technical University; 2015 [Doctoral dissertation].
[3] Liu CJ, Qi J, Jiang MF. Experimental study on sulfuric acid leaching behavior of chromite with different temperature. Adv Mater Res 2011;361–363:628–31, http://dx.doi.org/10.4028/www.scientific.net/amr.361-363.628.
[4] Mohanty U, Rintala L, Halli P, Taskinen P, Lundström M. Hydrometallurgical approach for leaching of metals from copper rich side stream originating from base metal production. Metals 2018;8(1):40, http://dx.doi.org/10.3390/met8010040.
[5] Tzeferis PG, Agatzini-Leonardou S. Leaching of nickel and iron from Greek non-sulphide nickeliferous ores by organic acids. Hydrometallurgy 1994;36(3):345–60, http://dx.doi.org/10.1016/0304-386X(94)90031-0.
[6] Ige J, Akanni MS, Morakinyo MK, Owoyomi O. A kinetic study of the leaching of iron and manganese from a Nigerian tantalite-columbite ore. J Appl Sci 2005;5(3):496–502, http://dx.doi.org/10.3923/jas.2005.496.502.
[7] Bar D, Barket ELD. Leaching of metals from hydrometallurgical residue by sulfuric acid. Aspects Mining Miner Sci 2018;1(4), http://dx.doi.org/10.31031/AMMS.2018.01.000518.
[8] Ni'am AC, Wang YF, Chen SW, You SJ. Recovery of rare earth elements from waste permanent magnet (WPMs) via selective leaching using the Taguchi method. J Taiwan Inst Chem Eng 2019;97:137–45, http://dx.doi.org/10.1016/j.jtice.2019.01.006.
[9] Mondal S, Paul B, Kumar V, Singh DK, Chakravartty JK. Parametric optimization for leaching of cobalt from Sukinda ore of lateritic origin – a Taguchi approach. Sep Purif Technol 2015;156:827–34, http://dx.doi.org/10.1016/j.seppur.2015.11.007.
[10] Behnajady B, Moghaddam J, Behnajady MA, Rashchi F. Determination of the optimum conditions for the leaching of lead from zinc plant residues in NaCl-H_2SO_4-$Ca(OH)_2$ media by the Taguchi Method. Ind Eng Chem Res 2012;51(10):3887–94, http://dx.doi.org/10.1021/ie202571x.
[11] Sharma S, Agarwal GK, Dutta NN. Kinetic study on leaching of Zn and Cu from spent low-temperature shift catalyst ($CuO/ZnO/Al_2O_3$): application of Taguchi design. J Mater Cycles Waste Manage 2020:1–12, http://dx.doi.org/10.1007/s10163-020-01038-x.
[12] Montgomery DC. Design and analysis of experiments. New York: Springer; 2019.
[13] Pundir R, Chary GHVC, Dastidar MG. Application of Taguchi method for optimizing the process parameters for the removal of copper and nickel by growing *Aspergillus* sp. Water Resour Ind 2018;20:83–92, http://dx.doi.org/10.1016/j.wri.2016.05.001.
[14] Liu JJ, Hu GR, Du K, Peng ZD, Cao YB. Influencing factors and kinetics analysis of a new clean leaching process for producing chromate from Cr-Fe alloy. J Clean Prod 2014;84:746–51, http://dx.doi.org/10.1016/j.jclepro.2014.01.062.
[15] Oktor K. Determination of Cr (VI) in creeks discharge to İzmit Gulf (Kocaeli, Turkey). J Sci Perspect 2019;3(3):201–6, http://dx.doi.org/10.26900/jsp.3.020.
[16] Shashanka R, Chaira D. Optimization of milling parameters for the synthesis of nano-structured duplex and ferritic stainless steel powders by high energy planetary milling. Powder Technol 2015;278:35–45, http://dx.doi.org/10.1016/j.powtec.2015.03.007.
[17] Ge X, Jin S, Zhang M, Wang X, Seetharaman S. Synthesis of chromium and ferrochromium alloy in molten salts by the electro-reduction method. J Mining Metall B Metall 2015;51(2):185–91, http://dx.doi.org/10.2298/jmmb141222022g.
[18] Neizel BW, Beukes JP, Van Zyl PG, Dawson NF. Why is $CaCO_3$ not used as an additive in the pelletised chromite pre-reduction process? Miner Eng 2013;45:115–20, http://dx.doi.org/10.1016/j.mineng.2013.02.015.
[19] Leško A, Navara E. Microstructural characterization of high-carbon ferrochromium. Mater Charact 1996;36(4–5):349–56, http://dx.doi.org/10.1016/S1044-5803(96)00068-X.
[20] Maslyuk VA, Bondar AA, Pidoprygora MI, Varchenko VM. Structure and properties of iron-high-carbon ferrochrome powder composites. Powder Metall Metal Ceram 2013;52(5–6):291–7, http://dx.doi.org/10.1007/s11106-013-9525-7.
[21] Agarwal S, Pal J, Ghosh D. Smelting characteristics of fluxed chromite sinter and its performance assessment in electric arc furnace to produce high carbon ferrochrome. Ironmaking Steelmaking 2016;43(2):97–111, http://dx.doi.org/10.1179/1743281215Y.0000000054.
[22] Capilla AV, Delgado AV. Thanatia: the destiny of the earth's mineral resources – a thermodynamic cradle-to-cradle assessment. World Scientific; 2014.
[23] Nadirov R, Mussapyrova L. Effect of mechanical activation on leachability of fayalite in sulfuric acid solution; 2020, http://dx.doi.org/10.2174/1877946810666200128152729.
[24] Salmimies R, Mannila M, Kallas J, Häkkinen A. Acidic dissolution of magnetite: experimental study on the effects of acid concentration and temperature. Clays Clay Miner 2011;59(2):136–46, http://dx.doi.org/10.1346/CCMN.2011.0590203.
[25] Kuznetsov VV, Pavlov LN, Vinokurov EG, Filatova EA, Kudryavtsev VN. Corrosion resistance of Cr-C-W alloys

produced by electrodeposition. J Solid State Electrochem 2015;19(9):2545–53, http://dx.doi.org/10.1007/s10008-015-3007-4.
[26] Havlik T, Turzakova M, Stopic S, Friedrich B. Atmospheric leaching of EAF dust with diluted sulphuric acid. Hydrometallurgy 2005;77(1–2):41–50, http://dx.doi.org/10.1016/j.hydromet.2004.10.008.
[27] Önal MAR, Aktan E, Borra CR, Blanpain B, Van Gerven T, Guo M. Recycling of NdFeB magnets using nitration, calcination and water leaching for REE recovery. Hydrometallurgy 2017;167:115–23, http://dx.doi.org/10.1016/j.hydromet.2016.11.006.
[28] Cruells M, Roca A, Núnẽz C. Electric arc furnace flue dusts: characterization and leaching with sulphuric acid. Hydrometallurgy 1992;31(3):213–31, http://dx.doi.org/10.1016/0304-386X(92)90119-K.
[29] Vitale RJ, Mussoline GR, Petura JC, James BR. Cr (VI) soil analytical method: a reliable analytical method for extracting and quantifying Cr (VI) in soils. Soil Sediment Contam 1997;6(6):581–93, http://dx.doi.org/10.1080/15320389709383591.
[30] Geveci A, Topkaya Y, Ayhan E. Sulfuric acid leaching of Turkish chromite concentrate. Miner Eng 2002;15(11):885–8, http://dx.doi.org/10.1016/S0892-6875(02)00159-0.
[31] Zhang B, Shi P, Jiang M. Advances towards a clean hydrometallurgical process for chromite. Minerals 2016;6(1):7, http://dx.doi.org/10.3390/min6010007.
[32] Moghaddam J, Sarraf-Mamoory R, Abdollahy M, Yamini Y. Purification of zinc ammoniacal leaching solution by cementation: determination of optimum process conditions with experimental design by Taguchi's method. Sep Purif Technol 2006;51(2):157–64, http://dx.doi.org/10.1016/j.seppur.2006.01.012.
[33] Lymperopoulou T, Georgiou P, Tsakanika LA, Hatzilyberis K, Ochsenkuehn-Petropoulou M. Optimizing conditions for scandium extraction from bauxite residue using Taguchi methodology. Minerals 2019;9(4):236, http://dx.doi.org/10.3390/min9040236.
[34] Copur M, Kizilca M, Kocakerim MM. Determination of the optimum conditions for copper leaching from chalcopyrite concentrate ore using Taguchi method. Chem Eng Commun 2015;202(7):927–35, http://dx.doi.org/10.1080/00986445.2014.891506.
[35] Zhao Q, Liu C, Shi P, Zhang B, Jiang M, Zhang Q, Saxen H, Zevenhoven R. Sulfuric acid leaching of South African chromite. Part 1: study on leaching behavior. Int J Miner Process 2014;130:95–101, http://dx.doi.org/10.1016/j.minpro.2014.04.002.
[36] Jiang M, Zhao Q, Liu C, Shi P, Zhang B, Yang D, Saxen H, Zevenhoven R. Sulfuric acid leaching of South African chromite. Part 2: optimization of leaching conditions. Int J Miner Process 2014;130:102–7, http://dx.doi.org/10.1016/j.minpro.2014.05.009.
[37] Aracena A, Fernández F, Jerez O, Jaques A. Converter slag leaching in ammonia medium/column system with subsequent crystallisation with NaSH. Hydrometallurgy 2019;188:31–7, http://dx.doi.org/10.1016/j.hydromet.2019.06.006.
[38] Teja Ruiz AM, Juárez Tapia JC, Reyes Domínguez IA, Hernández Cruz LE, Pérez MR, Patiño Cardona F, Flores Guerrero MU. Kinetic study of Ag leaching from arsenic sulfosalts in the S_2O_{32}-O_2-NaOH system. Metals 2017;7(10):411, http://dx.doi.org/10.3390/met7100411.
[39] Sokić MD, Marković B, Živković D. Kinetics of chalcopyrite leaching by sodium nitrate in sulphuric acid. Hydrometallurgy 2009;95(3–4):273–9, http://dx.doi.org/10.1016/j.hydromet.2008.06.012.
[40] Mulak W, Miazga B, Szymczycha A. Kinetics of nickel leaching from spent catalyst in sulphuric acid solution. Int J Miner Process 2005;77(4):231–5, http://dx.doi.org/10.1016/j.minpro.2005.06.005.
[41] Gireesh VS, Vinod VP, Nair SK, Ninan G. Effect of sulphate ions on leaching of ilmenite with hydrochloric acid. J Acad Ind Res 2013;2(7):402.
[42] Georgiou D, Papangelakis VG. Sulphuric acid pressure leaching of a limonitic laterite: chemistry and kinetics. Hydrometallurgy 1998;49(1–2):23–46, http://dx.doi.org/10.1016/S0304-386X(98)00023-1.
[43] Padilla R, Pavez P, Ruiz MC. Kinetics of copper dissolution from sulfidized chalcopyrite at high pressures in H_2SO_4-O_2. Hydrometallurgy 2008;91(1–4):113–20, http://dx.doi.org/10.1016/j.hydromet.2007.12.003.
[44] Şen Z. Innovative trend methodologies in science and engineering. New York: Springer; 2017. p. 56.
[45] Aydogan S, Aras A, Canbazoglu M. Dissolution kinetics of sphalerite in acidic ferric chloride leaching. Chem Eng J 2005;114(1–3):67–72, http://dx.doi.org/10.1016/j.cej.2005.09.005.